ORAL/POSTER REFERENCE: ICF1001006PR

AN INTEGRATED EFGM-FEM FOR LINEAR-ELASTIC FRACTURE MECHANICS

B. N. Rao and S. Rahman

College of Engineering, The University of Iowa,
Iowa City, IA 52242

ABSTRACT

This paper presents a method for integrating the element-free Galerkin method (EFGM) with the traditional finite element method (FEM) for analyzing linear-elastic cracked structures. The EFGM is used to model material behavior close to cracks and the FEM in areas away from cracks. In the interface region, the resulting shape function, which comprises both EFGM and FEM shape functions, satisfies the consistency condition thus ensuring convergence of the method. Numerical examples are presented to illustrate the integrated EFGM-FEM. The stress-intensity factors predicted by this method compare very well with all-FEM or all-EFGM solutions. A significant saving of computational effort can be achieved due to coupling in the proposed method when compared with existing meshless methods.

KEYWORDS

Element-free Galerkin method, finite element method, fracture, stress-intensity factor, crack propagation.

INTRODUCTION

In recent years, a class of meshfree or meshless methods, such as the element-free Galerkin method (EFGM) [1,2], has emerged that demonstrates significant potential for solving moving boundary problems typified by growing cracks. Although meshless methods are attractive for simulating crack propagation, the computational cost of a meshless method typically exceeds the cost of a regular finite element method (FEM). Furthermore, given the level of maturity and comprehensive capabilities of FEM, it is often advantageous to use meshless methods only in sub-domains, where their capabilities can be exploited to the greatest benefit. In modeling crack propagation in a complex engineering structure with stiffeners, connections, welds, *etc.*, it is more effective to apply meshless methods at sites of potential crack growth and FEM in the remainder of the domain. Therefore, numerical methods need to be developed for combining meshless and finite element methods.

In this paper, a numerical technique integrating EFGM with the traditional FEM is presented for analyzing linear-elastic cracked structures. The EFGM is used to model material behavior close to cracks and the FEM in areas away from cracks. In the interface region, the resulting shape function, which comprises both EFGM and FEM shape functions, satisfies the consistency condition thus ensuring convergence of the method. Several numerical examples are presented to illustrate the proposed method.

THE ELEMENT-FREE GALERKIN METHOD

Consider a function $u(\boldsymbol{x})$ over a domain $\Omega \subseteq \Re^K$, where K = 1, 2, or 3. Let $\Omega_x \subseteq \Omega$ denote a sub-domain describing the neighborhood of a point $\boldsymbol{x} \in \Re^K$ located in Ω. According to the moving least-squares (MLS) [3], the approximation $u^h(\boldsymbol{x})$ of $u(\boldsymbol{x})$ is

$$u^h(\boldsymbol{x}) = \sum_{I=1}^{N} \Phi_I(\boldsymbol{x}) d_I = \boldsymbol{\Phi}^T(\boldsymbol{x})\boldsymbol{d} \tag{1}$$

where $\boldsymbol{d}^T = \{d_1, \cdots, d_N\}$ and $\boldsymbol{\Phi}^T(\boldsymbol{x}) = \{\Phi_1(\boldsymbol{x}), \cdots, \Phi_N(\boldsymbol{x})\}$ with d_I representing the nodal parameter for node I and $\Phi_I(\boldsymbol{x}) = \boldsymbol{a}^T(\boldsymbol{x})\boldsymbol{p}(\boldsymbol{x}_I) w_I(\boldsymbol{x})$ representing the MLS shape function corresponding to node I, $\boldsymbol{a}(\boldsymbol{x})$ is a vector of unknown parameters, which can be determined by imposing reproducibility or consistency conditions, $\boldsymbol{p}^T(\boldsymbol{x}) = \{p_1(\boldsymbol{x}), p_2(\boldsymbol{x}), \cdots, p_m(\boldsymbol{x})\}$ is a vector of complete basis functions of order m, $w_I(\boldsymbol{x})$ is a weight function associated with node I such that $w_I(\boldsymbol{x}) \geq 0$ for all $\boldsymbol{x}$ in the support Ω_x of $w_I(\boldsymbol{x})$ and zero where $\boldsymbol{x}_I$ denotes the coordinates of node I, and N is the total number of meshless nodes. According to the reproducibility condition,

$$\boldsymbol{p}(\boldsymbol{x}) = \sum_{I=1}^{N} \boldsymbol{p}(\boldsymbol{x}_I)\Phi_I(\boldsymbol{x}) = \sum_{I=1}^{N} \boldsymbol{p}(\boldsymbol{x}_I)\Phi_I{}^T(\boldsymbol{x}) \tag{2}$$

Substituting $\Phi_I(\boldsymbol{x})$ in Equation 2 gives,

$$\boldsymbol{p}(\boldsymbol{x}) = \left[\sum_{I=1}^{N} \boldsymbol{p}(\boldsymbol{x}_I)\boldsymbol{p}^T(\boldsymbol{x}_I) w_I(\boldsymbol{x})\right] \boldsymbol{a}(\boldsymbol{x}). \tag{3}$$

INTEGRATED EFGM-FEM

Consider the domain $\Omega = \Omega_{EFGM} \cup \Omega_{FEM}$, which comprises two non-overlapping subdomains Ω_{EFGM} and Ω_{FEM} and boundary Γ_b. Depending the location of a point $\boldsymbol{x} \in \Re^K$, the reproducibility condition given by Equation 3 can be written as follows:

Case 1: If $\boldsymbol{x} \in \Omega_{EFGM}$ and the shape function of all FEM nodes are zero at $\boldsymbol{x}$,

$$\boldsymbol{p}(\boldsymbol{x}) = \sum_{I=1,\, \boldsymbol{x}_I \in \Omega_{EFGM}}^{N} \boldsymbol{p}(\boldsymbol{x}_I)\Phi_I(\boldsymbol{x}). \tag{4}$$

Case 2: If $\boldsymbol{x} \in \Omega_{EFGM}$ and the shape function of some FEM nodes along boundary Γ_b are nonzero at $\boldsymbol{x}$,

$$\boldsymbol{p}(\boldsymbol{x}) = \sum_{I=1,\, \boldsymbol{x}_I \in \Omega_{EFGM}}^{N} \boldsymbol{p}(\boldsymbol{x}_I)\Phi_I(\boldsymbol{x}) + \sum_{J=1,\, \boldsymbol{x}_J \in \Gamma_b}^{M} \boldsymbol{p}(\boldsymbol{x}_J) N_J(\boldsymbol{x}). \tag{5}$$

A node on the boundary between EFGM zone and FEM zone Γ_b is treated as an FEM node if its FEM shape function value at the point $\boldsymbol{x}$ is nonzero or else it is treated as EFGM Node. In this case,

$$\boldsymbol{p}(\boldsymbol{x}) = \boldsymbol{A}(\boldsymbol{x})\boldsymbol{a}(\boldsymbol{x}) + \sum_{J=1,\, \boldsymbol{x}_J \in \Omega_{FEM}}^{M} \boldsymbol{p}(\boldsymbol{x}_J) N_J(\boldsymbol{x}). \tag{6}$$

Case 3: If $\boldsymbol{x} \in \Omega_{FEM}$,

$$\boldsymbol{p}(\boldsymbol{x}) = \sum_{J=1,\, \boldsymbol{x}_J \in \Omega_{FEM}}^{M} \boldsymbol{p}(\boldsymbol{x}_J) N_J(\boldsymbol{x}), \tag{7}$$

where the FEM shape function $N_J(\boldsymbol{x})$ can be obtained by Lagrange interpolation. Hence, the effective shape function for integrated EFGM-FEM, denoted by $\tilde{\Phi}_I(\boldsymbol{x})$, can be defined as

$$\tilde{\Phi}_I(\boldsymbol{x}) = \begin{cases} \Phi_I(\boldsymbol{x}), & \text{if } \boldsymbol{x}_I \in \Omega_{EFGM} \\ N_I(\boldsymbol{x}), & \text{if } \boldsymbol{x}_I \in \Gamma_b \text{ and } N_I(\boldsymbol{x}) \neq 0 \\ \left\{ \boldsymbol{p}(\boldsymbol{x}) - \sum_{J=1,\, \boldsymbol{x}_J \in \Omega_{FEM}}^{M} \boldsymbol{p}(\boldsymbol{x}_J) N_J(\boldsymbol{x}) \right\}^T & \\ \boldsymbol{A}^{-1}(\boldsymbol{x}) \boldsymbol{p}(\boldsymbol{x}_I) w_I(\boldsymbol{x}), & \text{if } \boldsymbol{x}_I \in \Gamma_b \text{ and } N_I(\boldsymbol{x}) = 0 \\ N_I(\boldsymbol{x}), & \text{if } \boldsymbol{x}_I \in \Omega_{FEM} \end{cases} . \tag{8}$$

The effective shape function $\tilde{\Phi}_I(\boldsymbol{x})$ strongly depends on the type of basis functions used. In this study, the fully enriched basis function was used for analyzing cracked structures [1,2].

VARIATIONAL FORMULATION AND DISCRETIZATION

For small displacements in two-dimensional, homogeneous, isotropic, and linear-elastic solids, the variational or weak form of equilibrium equation is

$$\int_\Omega \boldsymbol{\sigma}^T \delta\boldsymbol{\epsilon} d\Omega - \int_\Omega \boldsymbol{b}^T \delta\boldsymbol{u} d\Omega - \int_{\Gamma_t} \bar{\boldsymbol{t}}^T \delta\boldsymbol{u} d\Gamma - \delta W_u = 0 \tag{9}$$

$$\delta W_u = \sum_{\boldsymbol{x}_J \in \Gamma_u} \delta\boldsymbol{f}^T(\boldsymbol{x}_J)\left[\boldsymbol{u}(\boldsymbol{x}_J) - \bar{\boldsymbol{u}}(\boldsymbol{x}_J)\right] + \boldsymbol{f}^T(\boldsymbol{x}_J)\delta\boldsymbol{u}(\boldsymbol{x}_J) \tag{10}$$

where $\boldsymbol{\sigma}$ is the stress vector, $\boldsymbol{\epsilon}$ is the strain vector, $\boldsymbol{u}$ is the displacement vector, $\boldsymbol{b}$ is the body force vector, and $\bar{\boldsymbol{t}}$ and $\bar{\boldsymbol{u}}$ are the vectors of prescribed surface tractions and displacements, respectively. Using the integrated EFGM-FEM method, the displacement field can be approximated by

$$u_i^h(\boldsymbol{x}_J) = \sum_{I=1}^{N} \tilde{\Phi}_I(\boldsymbol{x}_J) d_I^{\,i} = \tilde{\boldsymbol{\Phi}}_J^{\,iT} \boldsymbol{d} \tag{11}$$

where $\tilde{\boldsymbol{\Phi}}_J^{\,iT}$ and $\boldsymbol{d}$ are vectors of integrated EFGM-FEM shape functions and nodal parameters displacements, respectively, and N is the total number of nodal points in Ω. For a single boundary constraint $\bar{u}_i(\boldsymbol{x}_J) = g_i(\boldsymbol{x}_J)$ applied at node J in the direction of x_i coordinate, when Equations 11 is invoked, the discretized form of Equations 9 and 10 becomes [2]

$$\begin{bmatrix} \boldsymbol{k} & \tilde{\boldsymbol{\Phi}}_J^{\,i} \\ \tilde{\boldsymbol{\Phi}}_J^{\,iT} & 0 \end{bmatrix} \begin{Bmatrix} \boldsymbol{d} \\ f_i(\boldsymbol{x}_J) \end{Bmatrix} = \begin{Bmatrix} \boldsymbol{f}^{ext} \\ g_i(\boldsymbol{x}_J) \end{Bmatrix} \tag{12}$$

where $\boldsymbol{k} \in \mathcal{L}\left(\Re^{2N} \times \Re^{2N}\right)$ is the stiffness matrix and $\boldsymbol{f}^{ext} \in \Re^{2N}$ is the force vector. When multiple boundary constraints are enforced, an augmented system of similar linear equation can be developed. The equilibrium equations can be solved using the method of Lagrange multipliers [1] or transformation methods [2].

COMPUTATIONAL FRACTURE MECHANICS

Consider a structure with a rectilinear crack of length 2*a* that is subjected to external stresses. Let K_I and K_{II} be the stress-intensity factors (SIFs) for mode-I and mode-II, respectively. The SIFs can be evaluated using the domain form of an interaction integral $M^{(1,2)}$, i.e.,

$$K_I = \frac{E'}{2} M^{(1,2)}, \tag{13}$$

where $E' = E$ for plane stress and $E' = E/(1-\nu^2)$ for plane strain, and

$$M^{(1,2)} = \int_A \left[\sigma_{ij}^{(1)} \frac{\partial u_i^{(2)}}{\partial x_1} + \sigma_{ij}^{(2)} \frac{\partial u_i^{(1)}}{\partial x_1} - W^{(1,2)} \delta_{1j} \right] \frac{\partial q}{\partial x_j} dA \tag{14}$$

where $W^{(1,2)}$ is the mutual strain energy from the actual mixed mode state for the given boundary conditions (superscript 1) and the super-imposed near-tip mode I auxiliary state (superscript 2), and *q* is another weight function chosen such that it is *unity* at the crack tip, *zero* along the boundary of the domain, and arbitrary elsewhere. Following similar considerations, K_{II} can be calculated from Equations 13-14, except that the near-tip mode II state is chosen as auxiliary state while computing $M^{(1,2)}$.

In order to simulate crack growth, the crack-path direction must be determined. There are a number of criteria available to predict the direction of crack trajectory. In this study, the crack-growth simulation is based on the maximum circumferential stress criterion [5]. When the values of K_I and K_{II} are known, the direction of crack-propagation can be easily solved using standard numerical procedures. Other criteria, which are not considered here, can be easily implemented into the proposed method.

NUMERICAL EXAMPLES

Example 1: Stationary Crack under Mixed-Mode

This example involves an edge-cracked plate in Figure 1, which is fixed at the bottom and subjected to far-field shear stress τ^{∞} = 1 unit applied on the top. The plate has length *L* = 16 units, width *W* = 7 units, and crack length *a* = 3.5 units. Figure 2 shows the domain discretization involving 324 uniformly spaced nodes, some of which are treated as meshless nodes and rest of them are treated as 4-noded quadrilateral finite elements. The elastic modulus and Poisson's ratio were 30×10^6 psi and 0.25, respectively. A plane strain condition was assumed.

Table 1 shows the predicted K_I and K_{II} for several values of L_{EFG}/L, where L_{EFG} is defined in Figure 2. The reference solutions for this problem are: $K_I = 34$ units and $K_{II} = 4.55$ units [6]. The predicted K_I and K_{II} values compare very well with the reference SIF values up to L_{EFG}/L = 6/14. However, the accuracy of the predicted values deteriorates and oscillates when $L_{EFG}/L \le 5/14$, possibly due to the smaller meshless zone. Figure 3 plots variation of CPU ratio, defined as the ratio of CPU time using integrated EFGM-FEM and CPU time using meshless method for the whole domain. It is evident from the plot that CPU time decreases with decrease in L_{EFG}/L, as expected. Hence combining meshless method with FEM can significantly reduce computational effort for solving fracture-mechanics problems.

Example 2: Experimental Validation of Crack Propagation

In this example, crack trajectories predicted by the proposed method are compared with the Pustejovsky's experimental data [7]. Pustejovsky performed a series of uniaxial tension tests on isotropic Titanium Ti-6Al-4V plates with oblique center-cracks of length 2*a* = 13.5 mm (0.53 inch) at $\gamma = 43^0$ and length 2*a* = 14.2 mm (0.56 inch) at $\gamma = 30^0$. The reported dimensions and material properties of the specimens were:

length, $2L$ = 304.8 mm (12 inches), width, $2W$ = 76.2 mm (3 inches), elastic modulus, E = 110 GPa (16,000 ksi) and Poisson's ratio, ν = 0.29. A far-field uniaxial tensile stress, σ^{∞} = 207 MPa (30 ksi) was applied on the top and the bottom of the specimen during meshless analysis. Figures 4 and 5 show the dimensions of the specimen and the meshless discretization, respectively. The domain discretization involves 1124 nodes, some of which are treated as meshless nodes and rest of them, are treated as 4-noded quadrilateral finite elements. A plane strain condition was assumed.

Figures 6 and 7 show the comparison of the predicted crack trajectories by using meshless method for the whole domain and by the proposed method when $L_{EFG} / L = 11/16$ and $7/16$, with the experimental data in a small region *ABCD* (see Figure 5) surrounding the crack. The results in Figure 6 corresponds to $2a$ = 13.5 mm (0.53 inch) and $\gamma = 43^0$ and the results in Figure 7 corresponds to $2a$ = 14.2 mm (0.56 inch) and $\gamma = 30^0$. The predicted crack trajectories by the proposed method are in good agreement with all-meshless results or the experimental data.

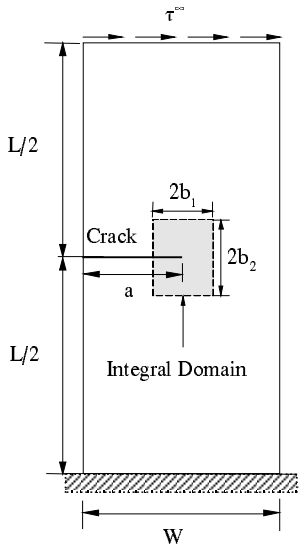

Figure 1. Edge-cracked plate

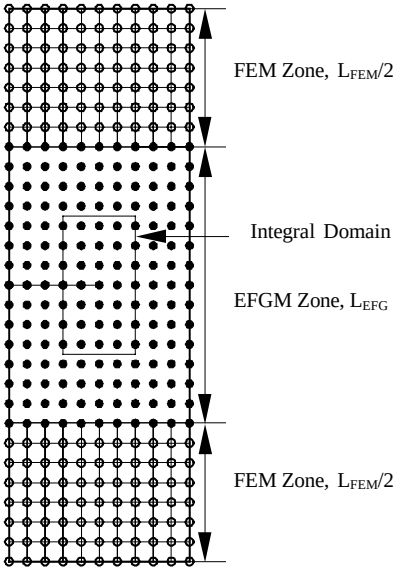

Figure 2. Domain discretization

TABLE 1
SIFs FOR EDGE-CRACKED PLATE

	Mode-I		Mode-II	
L_{EFG}/L	K_I	SIF Ratio[(a)]	K_{II}	SIF Ratio[(a)]
12/14	33.63	0.989	4.536	0.997
11/14	33.62	0.989	4.539	0.998
10/14	33.57	0.987	4.520	0.993
9/14	33.55	0.987	4.539	0.998
8/14	33.47	0.984	4.521	0.994
7/14	33.33	0.980	4.504	0.990
6/14	33.42	0.983	4.491	0.987
5/14	33.39	0.982	4.004	0.880
4/14	34.89	1.026	4.694	1.032
3/14	34.65	1.019	3.681	0.809
2/14	36.12	1.062	4.968	1.092

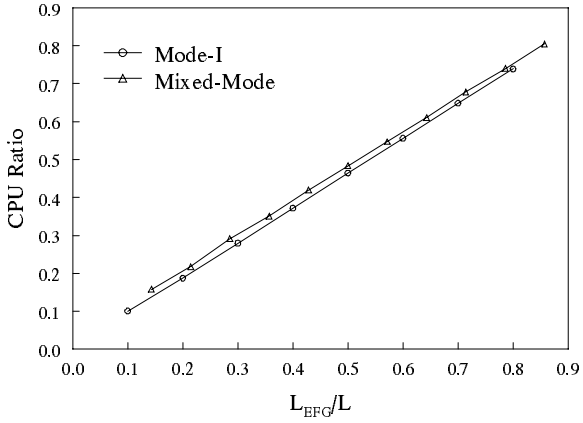

Figure 3. CPU time

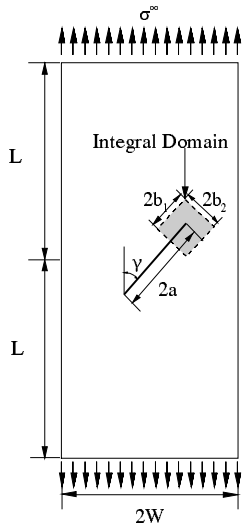

Figure 4. Angle-cracked plate

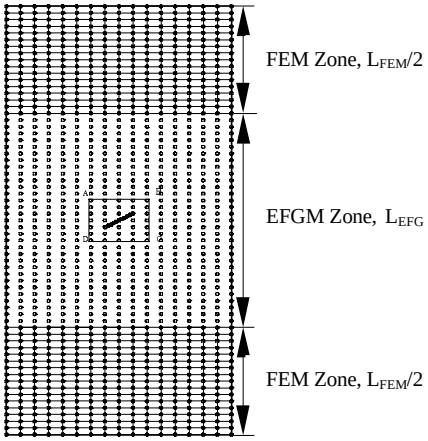

Figure 5. Domain discretization

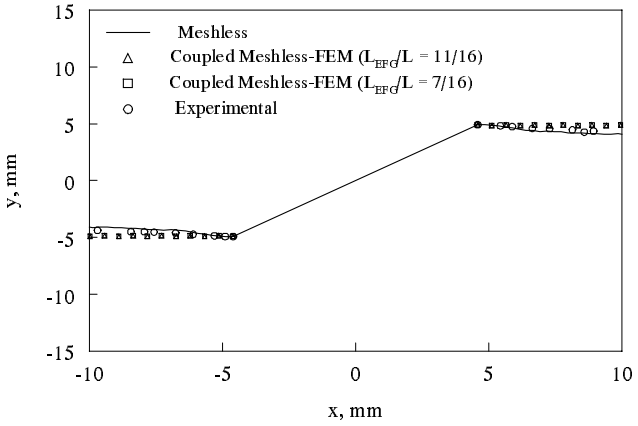

Figure 6. Crack propagation ($2a$ = 13.5 mm)

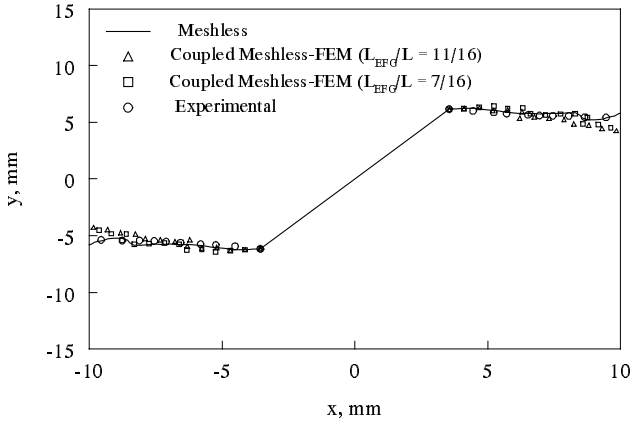

Figure 7. Crack propagation ($2a$ = 14.2 mm)

CONCLUSIONS

An integrated meshless-finite element method was developed for analyzing linear-elastic cracked structures subject to mixed-mode loading conditions. The EFGM was used to model material behavior close to cracks and the FEM in areas away from cracks. In the interface region, the resulting shape function, which comprises both EFGM and FEM shape functions, satisfies the consistency condition thus ensuring convergence of the method. Numerical examples show that the stress-intensity factors predicted by the proposed method compare very well with existing solutions obtained by all-FEM or all-EFGM analyses. A significant saving of computational effort can be achieved due to coupling in the proposed method when compared with existing meshless methods. The agreement between the predicted crack trajectories with those obtained from existing experimental data is excellent.

REFERENCES

1. Belytschko, T., Lu, Y., and Gu, L. (1995), *Engng. Frac. Mech.*, 51 (2), 295.
2. Rao, B. N., and Rahman, S. (2000), *Comp. Mech.*, 26, 398.
3. Lancaster, P. and Salkauskas, K. (1981), *Math. Comp.*, 37, 141.
4. Moran, B. and Shih,F. (1987), *Engng. Frac. Mech.*, 27, 615.
5. Erdogan, F. and Sih, G. C. (1963), *J. Basic Engng.*, 85, 519.
6. Wilson, W. K. (1969), *Ph.D. Thesis*, University of Pittsburgh, PA, USA.
7. Pustejovsky, M. A. (1979), *Engng. Frac. Mech.*, 11, 9.